Parasitology

cambridge.org/par

The dynamics of ultrastructural changes during *Entamoeba invadens* encystation

Eman Abdelazeem Abuelwafa Mousa[1,2,*], Miako Sakaguchi[3,4,*], Risa Nakamura[1,4], Osama Hussein Abdella[2], Hiroki Yoshida[5], Shinjiro Hamano[1,4] and Fumika Mi-ichi[5]

[1]Department of Parasitology, Institute of Tropical Medicine (NEKKEN), Nagasaki University, 1-12-4 Sakamoto, Nagasaki 852-8523, Japan; [2]Department of Medical Parasitology, Faculty of Medicine, South Valley University, Qena, Egypt; [3]Central Laboratory, Institute of Tropical Medicine (NEKKEN), Nagasaki University, 1-12-4 Sakamoto, Nagasaki 852-8523, Japan; [4]The Joint Usage/Research Center on Tropical Disease, Institute of Tropical Medicine (NEKKEN), Nagasaki University, 1-12-4 Sakamoto, Nagasaki 852-8523, Japan and [5]Division of Molecular and Cellular Immunoscience, Department of Biomolecular Sciences, Faculty of Medicine, Saga University, 5-1-1 Nabeshima, Saga 849-8501, Japan

Research Article

*These authors contributed equally to this work.

Cite this article: Mousa EAA, Sakaguchi M, Nakamura R, Abdella OH, Yoshida H, Hamano S, Mi-ichi F (2020). The dynamics of ultrastructural changes during *Entamoeba invadens* encystation. *Parasitology* **147**, 1305–1312. https://doi.org/10.1017/S0031182020001079

Received: 13 March 2020
Revised: 22 June 2020
Accepted: 1 July 2020
First published online: 14 July 2020

Key words:
Cell differentiation; dormancy; infectious disease; protozoan parasite

Authors for correspondence:
Fumika Mi-ichi,
E-mail: fumika@cc.saga-u.ac.jp,
Shinjiro Hamano,
E-mail: shinjiro@nagasaki-u.ac.jp

Abstract

Entamoeba histolytica infection causes amoebiasis, which is a global public health problem. The major route of infection is oral ingestion of *E. histolytica* cysts, cysts being the sole form responsible for host-to-host transmission. Cysts are produced by cell differentiation from proliferative trophozoites in a process termed 'encystation'. Therefore, encystation is an important process from a medical as well as a biological perspective. Previous electron microscopy studies have shown the ultrastructure of precysts and mature cysts; however, the dynamics of ultrastructural changes during encystation were ambiguous. Here, we analysed a series of *Entamoeba invadens* encysting cells by transmission electron microscopy. *Entamoeba invadens* is a model for encystation and the cells were prepared by short interval time course sampling from *in vitro* encystation-inducing cultures. We related sampled cells to stage conversion, which was monitored in the overall population by flow cytometry. The present approach revealed the dynamics of ultrastructure changes during *E. invadens* encystation. Importantly, the results indicate a functional linkage of processes that are crucial in encystation, such as glycogen accumulation and cyst wall formation. Hence, this study provides a reference for studying sequential molecular events during *Entamoeba* encystation.

Introduction

Entamoeba histolytica, a protozoan parasite belonging to the phylum Amoebozoa, is the causative agent for amoebiasis. Amoebiasis is a global public health problem owing to its high morbidity and mortality rates (Ralston and Petri, 2011; Watanabe and Petri, 2015). Most individuals infected with *E. histolytica* are asymptomatic and do not require medical treatment. However, asymptomatic individuals are important because they unconsciously spread the disease *via* cysts excreted in their feces. The principal source of amoebiasis is water or food contaminated by feces with mature cysts from infected individuals (Watanabe and Petri, 2015; Zulfiqar *et al.*, 2020). Currently, clinical options are inadequate; only a few drugs are available and an effective vaccine has not been developed (Quach *et al.*, 2014; Zulfiqar *et al.*, 2020).

Entamoeba histolytica survives drastic environmental changes outside as well as inside its human host by alternating its form between a proliferative trophozoite and a dormant cyst. The cyst is the sole form able to transmit the parasite to a new host. Cysts orally ingested by an individual can pass through the strong acidic conditions of the stomach to reach the small intestine where they hatch into trophozoites. This process is called excystation. Trophozoites then colonize the large intestine and proliferate there. Some of them differentiate into cysts in a process is called 'encystation'. Encystation is a parasitic strategy involving a fundamental cell differentiation process. This process is closely associated with the transmission of amoebiasis; therefore, inhibition of encystation is an effective strategy against amoebiasis (Mi-ichi *et al.*, 2016). Hence, *E. histolytica* encystation is an important subject from a medical as well as a biological perspective.

Entamoeba histolytica laboratory strains do not encyst after adaptation to *in vitro* cultures. However, studies using *in vitro E. histolytica* cultures have explored the conditions and chemicals that can induce the formation of cysts or cyst-like structures (Osada, 1959; Campos-Gongora *et al.*, 2000; Gonzalez-Salazar *et al.*, 2000; Said-Fernandez *et al.*, 2001; Aguilar-Díaz *et al.*, 2010). Meanwhile, *in vitro* culture of *Entamoeba invadens*, a reptilian parasite, has been used as a model system for encystation study (Eichinger, 1997; Mi-ichi *et al.*, 2016). Furthermore, the cysts formed in this model system can excyst to trophozoites (Mitra *et al.*, 2010; Suresh *et al.*, 2016). During *E. invadens* encystation, cell morphology changes; amoeboid cells become rounded dormant cells. Substantial changes occur concurrently in cell components. For example, a single nucleus becomes four and ribosomes become aggregated into chromatoid bodies (Tanyuksel and Petri, 2003). Chitins, a major component of the cyst wall, are synthesized and layered around the cell to resist environmental assault (Chatterjee *et al.*, 2009; Samanta and

© The Author(s) 2020. Published by Cambridge University Press

CAMBRIDGE UNIVERSITY PRESS

Ghosh, 2012; Samuelson *et al.*, 2013). Various *Entamoeba* encysting cell ultrastructures, such as precysts and mature cysts, have been observed by electron microscopy (Deutsch and Zaman, 1959; Osada, 1959; Proctor and Gregory, 1973; Eichinger, 1997; Chavez-Munguia *et al.*, 2003). However, it is difficult to predict the dynamics of ultrastructural changes during *Entamoeba* encystation by linking the results from different studies because a single time point sample was used in each study.

In this study, to overcome this limitation, we used transmission electron microscopy to analyse a series of samples collected over a short interval time course from an *in vitro* encystation-inducing *E. invadens* culture. The serial samples were also analysed by a flow cytometry method using premixed calcofluor (CF) and Evans blue (EB) dyes to confirm the progress of the encystation process (Mi-Ichi *et al.*, 2018).

Materials and methods

Parasite culture and sample preparations for electron microscopy and flow cytometry

In vitro cultures of *E. invadens* (IP-1) were routinely maintained, and cyst formation was induced as described (Mi-Ichi *et al.*, 2018). Briefly, *E. invadens* trophozoites suspended in encystation medium (6×10^5 cells mL^{-1}) were seeded in 96-well culture plates (240 μL per well) and sealed as described using PARAFILM® (Bemis Company, Inc., Oshkosh, WI) (Suresh *et al.*, 2016). Then plates were incubated at 26°C for the period indicated. Cells were pelleted by centrifuging the 96-well plates at the indicated time at 440 ***g*** for 5 min at 4°C.

For electron microscopy, cell pellets from 24 wells of a 96-well plate were collected in a single 1.5 mL tube using 1 mL phosphate-buffered saline (PBS), and were then centrifuged at 1330 ***g*** for 5 min at 4°C. The cell pellet was fixed with 2% glutaraldehyde (25% stock, Nacalai Tesque, Kyoto, Japan) in cacodylate buffer [0.1 M sodium cacodylate containing 1 mM $CaCl_2$ and 1 mM $MgCl_2$ (pH 7.4)] (vol/vol) with rotation for 60 min at 4°C. Cells were then rinsed with cacodylate buffer, and post-fixed with 1% OsO_4 (Nacalai Tesque) in cacodylate buffer (wt/vol) for 60 min at 4°C. They were then washed with cacodylate buffer and then dehydrated in a series of ethanol solutions [50, 70, 80 and 90% in deionized water (vol/vol)] followed by acetone solutions [90, 95 and 100% in deionized water (vol/vol)] for 5 min each. Cells were further dehydrated in anhydrous acetone for 40 min, incubated in propylene oxide for 10 min, and embedded in Quetol 651 epoxy resin (Nisshin EM, Tokyo, Japan). The resin-embedded samples were trimmed and sectioned using a diamond knife on an ultramicrotome (Reichert-Jung, Austria). Ultra-thin sections were collected on grids and stained with uranyl acetate and lead citrate. The resulting samples were examined at 80 kV under a transmission electron microscope (JEM-1230; JEOL, Tokyo, Japan). Cells showing ultrastructural characteristics were manually counted in randomly selected images (20 sections, each of which includes one cell, per sampling time).

For flow cytometry, cells pelleted in 96-well plates were treated and processed, and the obtained data were analysed as previously described (Mi-Ichi *et al.*, 2018).

Excystation was induced as described (Mitra *et al.*, 2010) with slight modification. In detail, encysted cells in 96-well plates were harvested 72 h post-induction by centrifugation, resuspended in sterile water (240 μL per well), and left at 26°C for 6 h to lyse trophozoites. Cells were then pelleted by centrifugation, resuspended in excystation medium (5 mg/mL bile and 40 mM sodium bicarbonate in LYI-S; 240 μL per well), and incubated at 26°C for 8 h. Excystation rates were determined by counting trophozoites *vs* total intact cells using a phase-contrast microscope.

Results

The dynamics of ultrastructural changes during E. invadens *encystation*

A series of transmission electron microscopy images were obtained from short interval time course samples of *in vitro* encystation-inducing *E. invadens* cultures. These images showed that at the 0 h time point, amoeboid cells with pseudopods were trophozoites, which were similar in structure to those described by (Proctor and Gregory, 1972) (0 h in Fig. 1), and that after 72 h, cells had become cysts, being surrounded by a thick wall (72 h in Fig. 1). The excysting rate was 55–60%. In addition, the images revealed remarkable ultrastructure, including nuclei (Deutsch and Zaman, 1959; Osada, 1959; Ludvik and Shipstone, 1970), chromatid bodies (Barker and Deutsch, 1958; Barker and Svihla, 1964), cyst walls (Chavez-Munguia *et al.*, 2007; Chavez-Munguia and Martinez-Palomo, 2011), cytoplasmic glycogen (Deutsch and Zaman, 1959; Osada, 1959) and vesicles (Osada, 1959; Proctor and Gregory, 1972) (see the sections below). These results indicate that the series of images reflects the process of *E. invadens* encystation. We also counted the number of cells showing these ultrastructural characteristics in randomly selected 20 sections, each of which includes a single cell, to know a profile of ultrastructural changes in the analysed samples (Supplementary Table 1). We then analysed the dynamics of the ultrastructural changes during *E. invadens* encystation.

These images were also related to changes in live cells, which were monitored as a population by a flow cytometry method (Mi-Ichi *et al.*, 2018) (Supplementary Fig. 1). The high specificities of the dyes used, EB and CF, which bind to the cell membrane and chitin, respectively, enabled the encystation process to be traced by monitoring the physiological and morphological changes. EB is an indicator of membrane permeability, whereas CF is an indicator of the synthesis and degradation of chitin polymers, the conformational change of the synthesized polymers or both. The flow cytometry results (Supplementary Fig. 1) were consistent with those of (Mi-Ichi *et al.*, 2018). For instance, the major CF^-/EB^+ population (proliferating trophozoites) moved to a CF^+/EB^- population (mature cysts) *via* CF^{low}/EB^+ and CF^+/EB^+ populations. CF^{low}/EB^{strong} and CF^+/EB^{strong} populations (abnormal cells) were also observed at much lower frequencies. This flow cytometry method also enabled the encystation efficiency to be determined (Mi-Ichi *et al.*, 2018); the present analyses were performed at 75–85% encystation efficiency.

Nucleus

The nucleus was observed throughout *E. invadens* encystation. The structure is very different from those of mammalian and yeast cells (Wright, 2000). Irregular outlines, the accumulation of many electron-dense chromatin granules under the nuclear membrane, and small central karyosomes were observed (0, 4 and 16 h in Figs 1 and 2A). These observations are consistent with (Osada, 1959). Because a single cell was analysed by a single section, not all nuclei are visible, but after 24 h, more than two nuclei per cell started to be seen (32–72 h in Figs 1 and 2B) (Supplementary Table 1). Therefore, nuclear multiplication started around 24 h post encystation induction. Tiny clear spots in chromatin granules (Fig. 2) are probably artefacts produced by the evaporation of substances due to high electron-density, as described by (Osada, 1959).

Vesicles

The cytoplasm of trophozoites was full of vesicles (0 h in Fig. 1). From 4 h, the number of vesicles in the cytoplasm gradually

https://doi.org/10.1017/S0031182020001079 Published online by Cambridge University Press

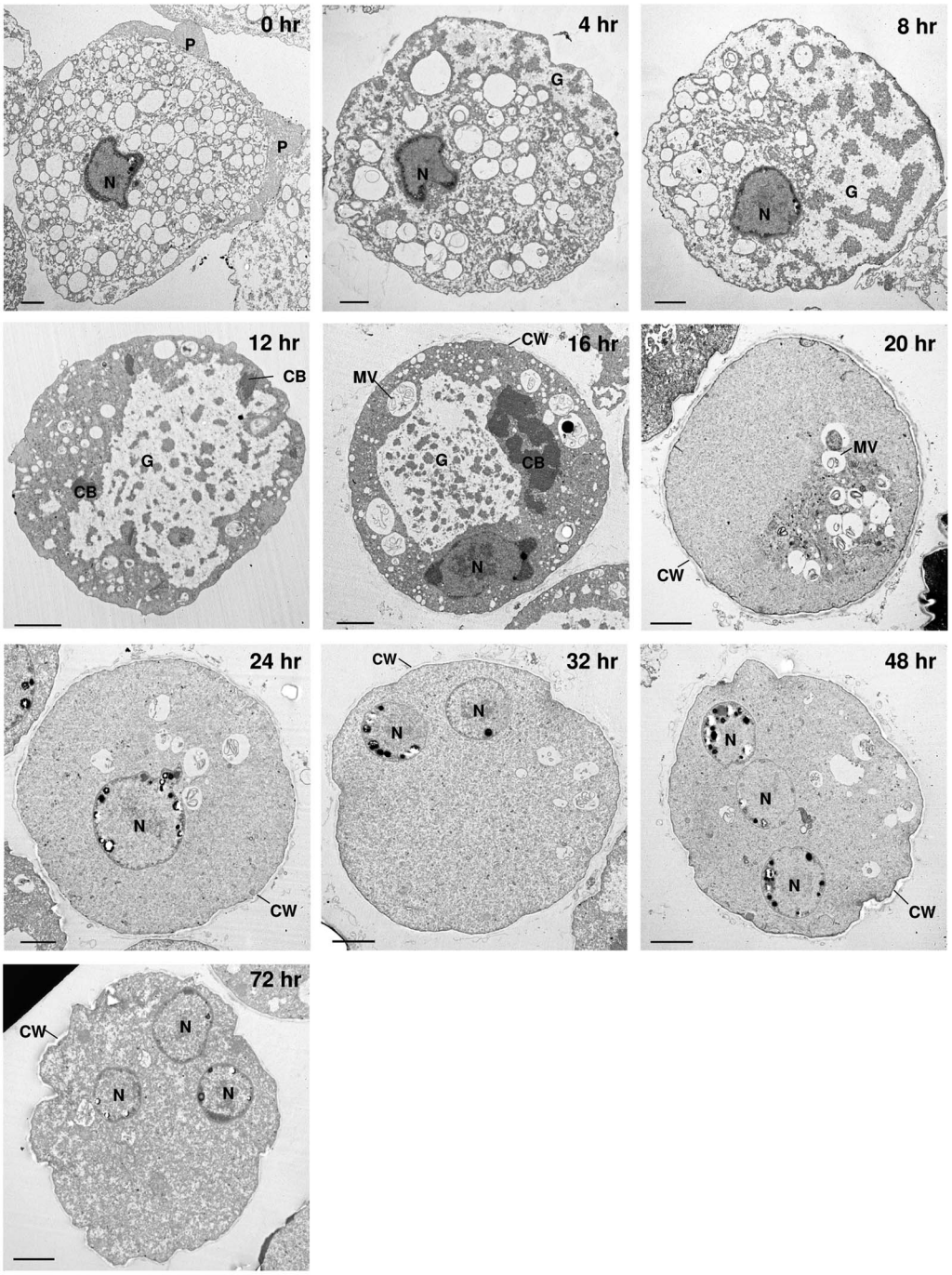


Fig. 1. Ultrastructure of *E. invadens* cells undergoing differentiation from trophozoites into cysts. Serial transmission electron microscopy images of encysting cells. The representative images are from more than 20 sections at each time point. Scale bar indicates 2 μm. CB, chromatoid body; CW, cyst wall; G, cytoplasmic glycogen; MV, multivesicular body; N, nucleus; P, pseudopodium; V, vesicle.

decreased with time, and almost no vesicles were observed at 72 h (4–72 h in Fig. 1). At 8 h, vesicles appeared to be more prevalent towards one side of a cell, and at 20 h, vesicles appeared to be have further congregated together (8 and 20 h in Fig. 1). From 12 h onwards, materials within vesicles became evident (20–72 h in Fig. 1; Supplementary Table 1). Some vesicles encompassed small vesicles (Fig. 3), which were similar to multivesicular bodies (Saito-Nakano *et al.*, 2004).

Autophagosome-like structures

Small structured vesicles involved in the sequestration of cytoplasmic contents (about 500 nm) were observed from 12 to 24 h (Fig. 4). These vesicles differ from multivesicular bodies and resemble autophagosomes in mammalian and yeast cells [Fig. 4, (Baba *et al.*, 1994)]. Interestingly, there are several genes annotated as autophagy components in *E. histolytica* and *E. invadens* genomes, and autophagy plays an important role in encystation (Picazarri *et al.*, 2008, 2015); however, whether these components are localized in the observed vesicles needs to be elucidated.

Cytoplasmic glycogen

Small accumulations of cytoplasmic glycogen, which are translucent non-geometric shaped regions without membranous

https://doi.org/10.1017/S0031182020001079 Published online by Cambridge University Press

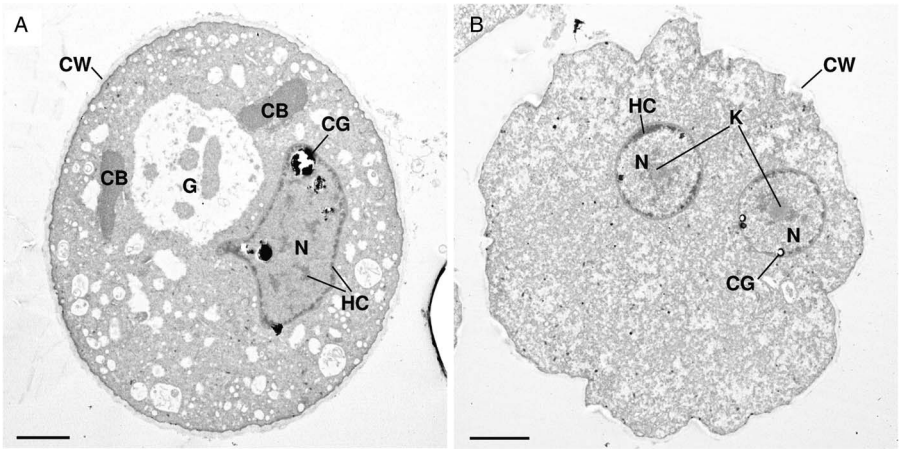


Fig. 2. The increasing number of nuclei in a single cell during *E. invadens* encystation. (A) An irregular nuclear shape in the encysting cell at 20 h. (B) Two nuclei in the cyst at 72 h. Scale bars indicate 2 μm. CB, chromatoid body; CG, chromatin granules; CW, cyst wall; G, cytoplasmic glycogen; HC, heterochromatin; K, karyosomes; N, nucleus.

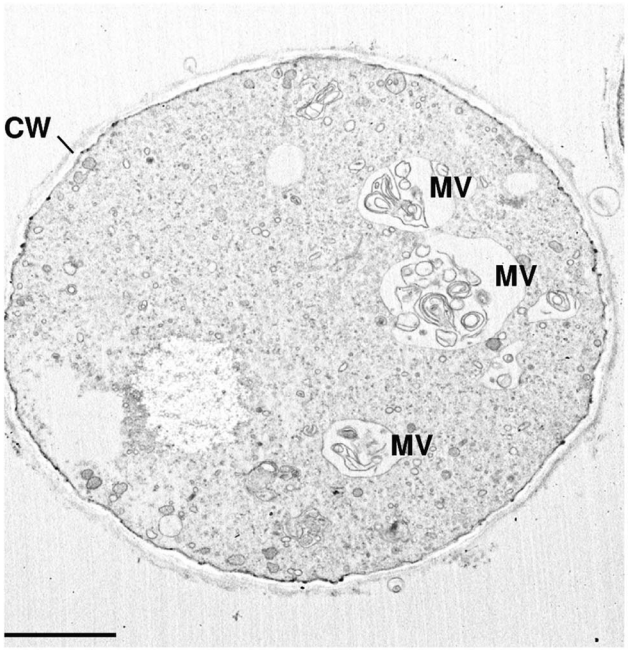


Fig. 3. Multivesicular bodies in the *E. invadens* encysting cell. The image is of an encysting cell at 32 h post-induction. Scale bar indicates 2 μm. CW, cyst wall; MV, multivesicular body.

boundaries (Deutsch and Zaman, 1959; Osada, 1959), were observed in trophozoites. The cytoplasmic glycogen, together with vesicles, almost entirely filled the cytoplasm of trophozoites (0 h in Fig. 1; Supplementary Table 1). From 4 h, glycogen scattered throughout the cytoplasm began to coalesce (Fig. 5A and B; Supplementary Table 1) and occupied almost half of the area of the cytoplasm at 8 h (4 and 8 h in Fig. 1). These structural changes of cytoplasmic glycogen are consistent with those described by (Osada, 1959). Notably, at 12 h, glycogen appeared to be have assembled into accumulated structures that were seen until 16 h (12 and 16 h in Figs 1 and 5C and D). From 24 h onwards, glycogen particles were not visible in most sections (Supplementary Table 1).

Chromatoid bodies

Chromatoid bodies are rod- or bar-shaped cellular inclusions thought to be composed of RNA and protein, but their exact function in *Entamoeba* cells remains elusive (Manna and Singh, 2019). Chromatoid bodies arise by the process of aggregation of small helical ribonucleoproteins (Siddiqui and Rudzinska, 1963). Up to 12 h, small chromatoid bodies of <2 nm in length were observed in the cytoplasm (Fig. 6A–D; Supplementary Table 1). From 12 h, larger forms of chromatoid bodies ⩾2 nm in length appeared and became most numerous between 16 and 20 h (Fig. 6E and F; Supplementary Table 1). Chromatoid bodies were frequently observed up to 20 h, but were rare from 32 h onwards (Supplementary Table 1).

Cyst walls

Fragmented electron-dense structures surrounding the surface of rounded cells were observed from 12 h (Fig. 7A–D). This structure is plausibly an intermediate appearing during the synthesis of the cyst wall. Cyst walls could be seen from 20 h onwards as previously described (Chavez-Munguia *et al.*, 2007; Chavez-Munguia and Martinez-Palomo, 2011). They have connected forms of the fragmented structures that became thick and coated the cell (Fig. 7E and F). Small cytoplasmic vesicles possessing granular material and located close to the plasma membrane were observed at 24 h (24 h in Fig. 1). These vesicular structures were similar to those reported in *E. histolytica* cysts (Chavez-Munguia and Martinez-Palomo, 2011).

Cyst wall formation can also be monitored by a flow cytometry method using two dyes, CF and EB (Mi-Ichi *et al.*, 2018). The profile of CF and EB signal changes is reproducible (Mi-Ichi *et al.*, 2018). The CF signal, the change of which reflected the amount of chitin and/or the confirmation of its polymer, stayed at a low level at 0–8 h. At 12 h, the signal shifted from a low level to a higher level, becoming obvious from 16 h. From 24 h onwards, the signal stabilized (Supplementary Fig. 1). This CF profile indicated that chitin synthesis started after 8 h and reached a maximum level at 16–24 h. This CF profile was consistent with the process of cyst wall formation observed by electron microscopy, where fragmented electron-dense structures on the cell surface became visible at 16 h and mature cyst walls were seen from 20 h onwards (Fig. 1; Supplementary Table 1). Taken together, the results indicate that cyst wall formation starts after 12 h and is completed within 20 h of encystation induction.

Discussion

Several electron microscopy studies have been published that show various ultrastructural features in encysting *E. invadens* and *E. histolytica* cells at a single time point (Deutsch and Zaman, 1959; Osada, 1959; Proctor and Gregory, 1973; Eichinger, 1997;

https://doi.org/10.1017/S0031182020001079 Published online by Cambridge University Press

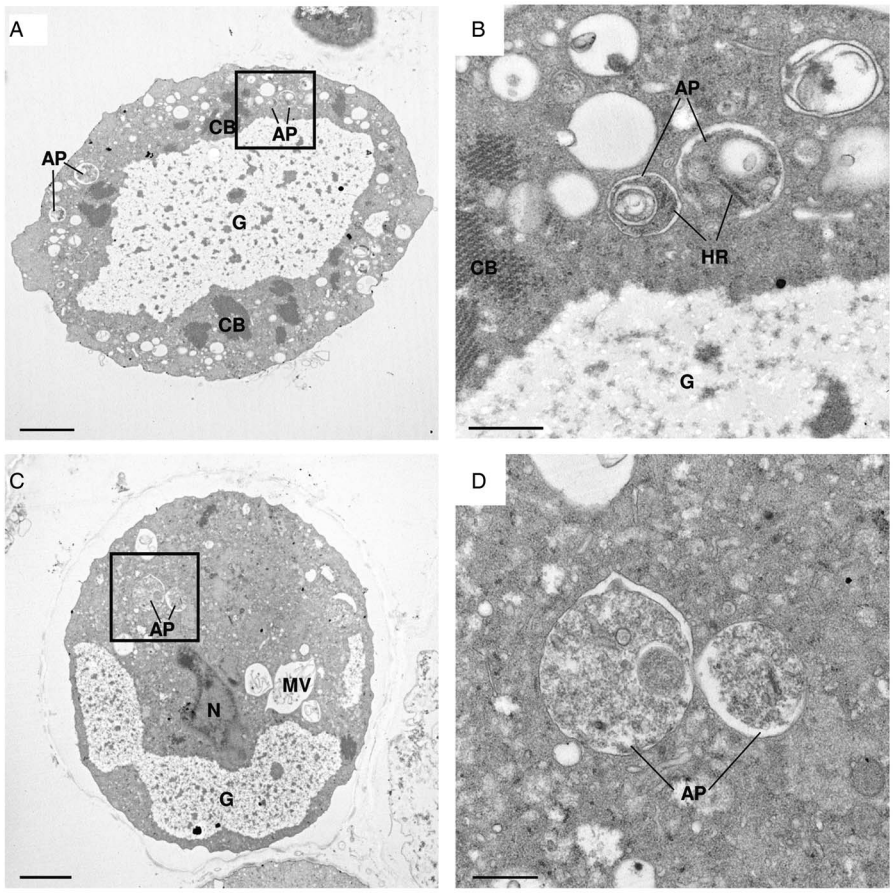


Fig. 4. Autophagosome-like structures in *E. invadens* encysting cells. (A, C) The images are of encysting cells. (B) An enlarged image of the boxed region in (A), which was obtained at 12 h post-induction. (D) An enlarged image of the boxed region in (C), which was obtained at 16 h post-induction. Scale bars in A and C indicate 2 μm, whereas those in B and D indicate 0.5 μm. AP, autophagosome-like structures; CB, chromatoid body; G, cytoplasmic glycogen; HR, helical ribonucleoprotein; MV, multivesicular body; N, nucleus.

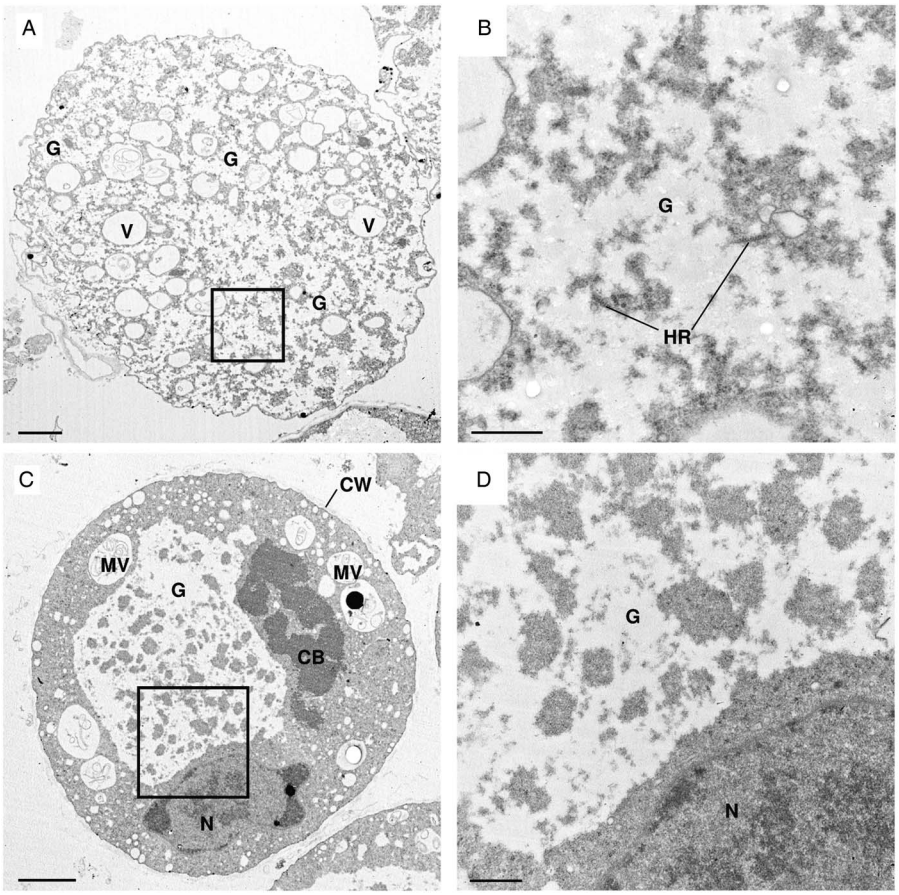


Fig. 5. Change of cytoplasmic glycogen form during *E. invadens* encystation. Glycogen scattered around the cytoplasm (A) coalesced (C) during encystation. (B) An enlarged image of the boxed region in (A), which was obtained at 4 h post-induction. (D) An enlarged image of the boxed region in (C), which was obtained at 16 h post-induction (the same image as Fig. 1, 16 h). Scale bars in A and C indicate 2 μm, whereas those in B and D indicate 0.5 μm. CB, chromatoid body; CW, cyst wall; HR, helical ribonucleoprotein; G, cytoplasmic glycogen; MV, multivesicular body; N, nucleus; V, vesicle.

https://doi.org/10.1017/S0031182020001079 Published online by Cambridge University Press

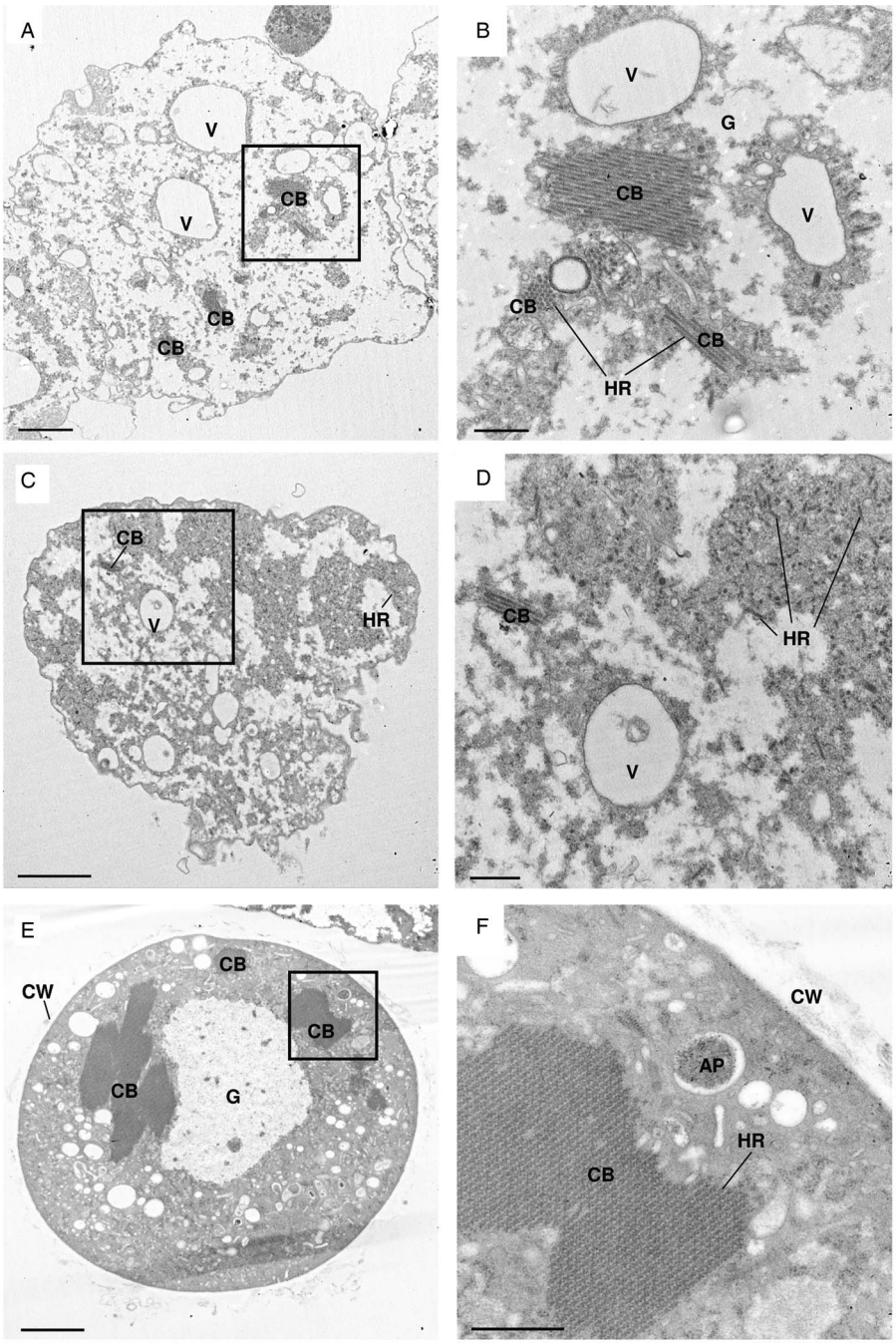


Fig. 6. Change of chromatoid body size during *E. invadens* encystation. (A, C) Chromatoid bodies of <2 nm in length at their longest point. (E) Chromatoid bodies ⩾2 nm in length at their longest point. (B) An enlarged image of the boxed region in (A), which was obtained at 4 h post-induction. (D) An enlarged image of the boxed region in (C), which was obtained at 8 h post-induction. (F) An enlarged image of the boxed region in (E), which was obtained at 12 h post-induction. Scale bars in A, C, and E indicate 2 μm, whereas those in B, D, and F indicate 0.5 μm. AP, autophagosome-like structures; CB, chromatoid body; CW, cyst wall; G, cytoplasmic glycogen; HR, helical ribonucleoprotein; V, vesicle.

Chavez-Munguia *et al.*, 2003). However, it is difficult to predict the dynamics of ultrastructural changes during *Entamoeba* encystation by combining the results from these different studies. Therefore, we performed a transmission electron microscopy analysis of a series of *E. invadens* encysting cells prepared from short interval time course samples of an *in vitro* culture. We revealed the dynamics of ultrastructure changes during *E. invadens* encystation. Furthermore, we combined a flow cytometry method to monitor the level of cell differentiation in a population of live cells (Mi-Ichi *et al.*, 2018). Our approach enabled us to refine the timing for cyst wall formation because the electron microscopy and flow cytometry monitored cyst wall formation from different perspectives. Electron microscopy traced structural changes of the cyst wall *per se*, whereas flow cytometry traced changes in live cells that reflected the process of cyst wall formation. The processes examined were the synthesis of a major component of the cyst wall, chitin, and the decrease of substance permeability.

Our results predict that cyst wall formation follows cytoplasmic glycogen disappearance. This sequence indicates the functional linkage of these two processes because cytoplasmic glycogen disappearance reflects the degradation of stored glycogen to provide a substrate for the synthesis of chitin. Glycogen hydrolysis provides D-glucose-1-phosphate *via* D-glucose, which is an essential substrate for the chitin synthetic pathway (Samanta and Ghosh, 2012). Intriguingly, in *E. histolytica*, the cyst-like structure formation was impaired by knockdown of the D-glucosamine 6-phosphate isomerase gene, which inhibits chitin synthesis (Aguilar-Díaz *et al.*, 2013).

Furthermore, the predicted timing of cyst wall formation, as described above, can be linked to the dynamics of other remarkable ultrastructure changes, such as nuclear division. The initiation of nuclear multiplication, which was observed by electron microscopy, occurs after cyst wall formation. This interpretation

https://doi.org/10.1017/S0031182020001079 Published online by Cambridge University Press

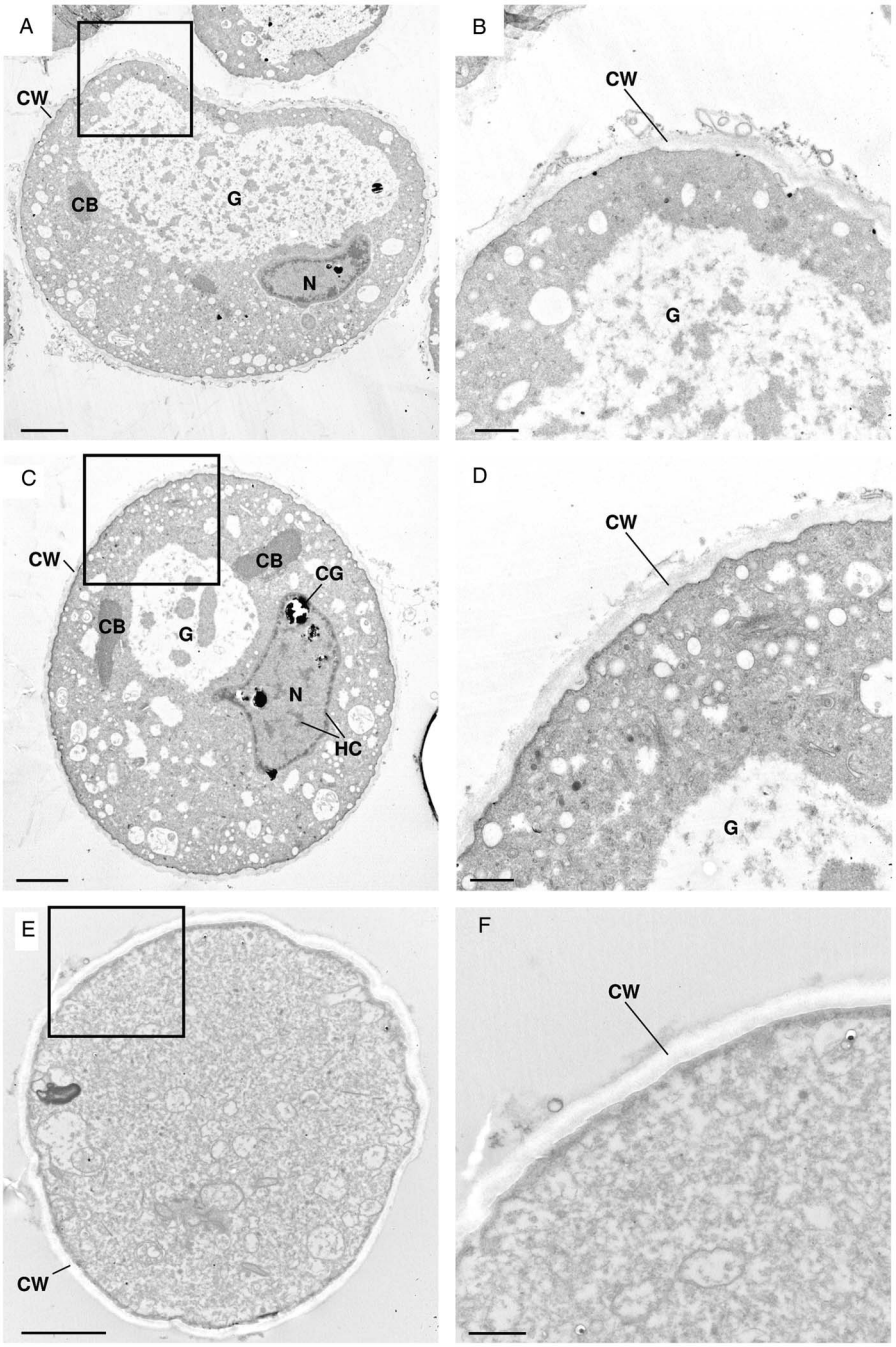


Fig. 7. Structural changes to cyst walls during *E. invadens* encystation. (A, C) Putative cyst wall intermediates. (E) Thick-coated cyst wall. (B) An enlarged image of the boxed region in (A), which was obtained at 16 h post-induction. (D) An enlarged image of the boxed region in (C), which was obtained at 20 h post-induction. The image shown in (C) is the same as Fig. 2A. (F) An enlarged image of the boxed region in (E), which was obtained at 150 h post-induction. Scale bars in A, C, and E indicate 2 μm, whereas those in B, D, and F indicate 0.5 μm. CB, chromatoid body; CG, chromatin granules; CW, cyst wall; G, cytoplasmic glycogen; HC, heterochromatin; N, nucleus.

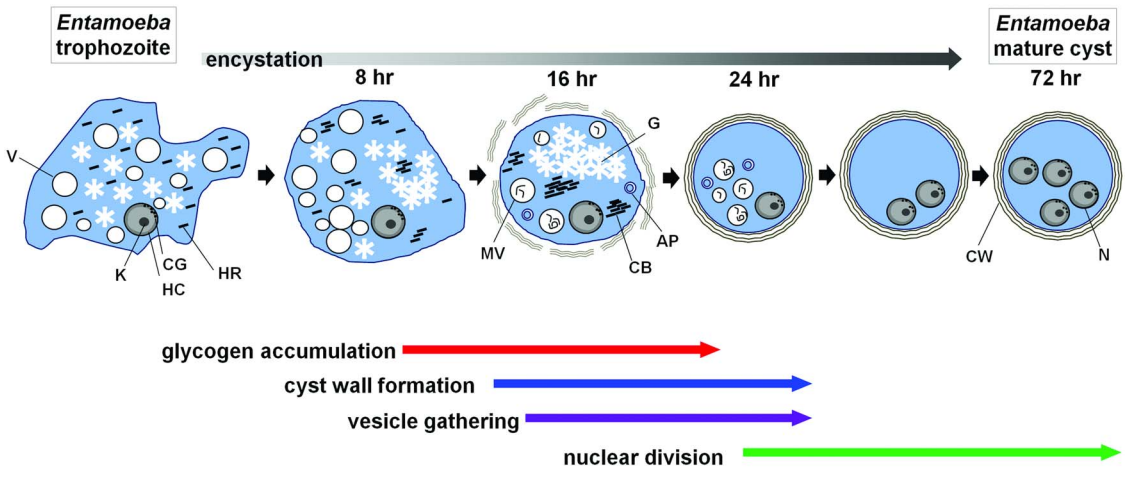


Fig. 8. Scheme showing the timing of ultrastructural changes during *E. invadens* encystation. Arrows indicate the period during which each ultrastructural change was observed. AP, autophagosome-like structures; CB, chromatoid body; CG, chromatin granules CW, cyst wall; G, cytoplasmic glycogen; HC, heterochromatin; HR, helical ribonucleoprotein; K, karyosomes; MV, multivesicular body; N, Nucleus; V, vesicle.

https://doi.org/10.1017/S0031182020001079 Published online by Cambridge University Press

is consistent with that of (Eichinger, 1997); nuclear division starts after the cyst wall has formed.

In conclusion, we showed the dynamics of cell component changes during *Entamoeba* encystation, and we predicted the sequence of the structural changes; glycogen accumulation precedes the cyst wall formation. On completing the cyst wall formation, multivesicular bodies and autophagosome-like structures become evident. After becoming a mature cyst, nuclear division occurs (see Fig. 8). Hence, the present study provides a reference for studying the sequential molecular events during *E. histolytica* as well as *E. invadens* encystation.

Supplementary material. The supplementary material for this article can be found at https://doi.org/10.1017/S0031182020001079.

Acknowledgements. This work was partly conducted at the Joint Usage/Research Center on Tropical Disease, Institute of Tropical Medicine, Nagasaki University. We thank Dr Sharmina Deloer, Ms. Ritsuko Yoshida, Ms. Minako Suzuki, and Ms. Mayuko Matsunaga for technical assistance. We thank Jeremy Allen, PhD, from Edanz Group (www.edanzediting.com/ac) for editing a draft of this manuscript.

Financial support. Eman Abdelazeem Abuelwafa Mousa received a PhD fellowship from The Egyptian Ministry of Higher Education. This work was supported by the Ministry of Education, Culture, Sports, Science and Technology of Japan (Grants-in-Aid for Scientific Research 18H04675 to F.M), AMED-J-PRIDE (JP19fm0208025 to H.Y., S.H. and F.M.), and the Joint Usage/Research Center on Tropical Disease, Institute of Tropical Medicine (NEKKEN), (2017-Ippan-12, 2018-Ippan-17, and 2020-Ippan-17 to F.M.).

Conflict of interest. None.

Ethical standards. Not applicable.

References

Aguilar-Díaz H, Díaz-Gallardo M, Laclette JP and Carrero JC (2010) In vitro induction of *Entamoeba histolytica* cyst-like structures from trophozoites. *PLoS Neglected Tropical Diseases* **4**, e607.

Aguilar-Díaz H, Laclette JP and Carrero JC (2013) Silencing of *Entamoeba histolytica* glucosamine 6-phosphate isomerase by RNA interference inhibits the formation of cyst-like structures. *Biomed Research International* **2013**, 758341.

Baba M, Takeshige K, Baba N and Ohsumi Y (1994) Ultrastructural analysis of the autophagic process in yeast: detection of autophagosomes and their characterization. *Journal of Cell Biology* **124**, 903–913.

Barker DC and Deutsch K (1958) The chromatoid body of *Entamoeba invadens*. *Experimental Cell Research* **15**, 604–610.

Barker DC and Svihla G (1964) Localization of cytoplasmic nucleic acid during growth and encystment of *Entamoeba invadens*. *Journal of Cell Biology* **20**, 389–398.

Campos-Gongora E, Viader-Salvado JM, Martinez-Rodriguez HG, Zuniga-Charles MA, Galindo JM and Said-Fernandez S (2000) Mg, Mn, and Co ions enhance the formation of *Entamoeba histolytica* cyst-like structures resistant to sodium dodecyl sulfate. *Archives of Medical Research* **31**, 162–168.

Chatterjee A, Ghosh SK, Jang K, Bullitt E, Moore L, Robbins PW and Samuelson J (2009) Evidence for a 'wattle and daub' model of the cyst wall of *Entamoeba*. *PLoS Pathogens* **5**, e1000498.

Chavez-Munguia B and Martinez-Palomo A (2011) High-resolution electron microscopical study of cyst walls of *Entamoeba* spp. *Journal of Eukaryotic Microbiology* **58**, 480–486.

Chavez-Munguia B, Cristobal-Ramos AR, Gonzalez-Robles A, Tsutsumi V and Martinez-Palomo A (2003) Ultrastructural study of *Entamoeba invadens* encystation and excystation. *Journal of Submicroscopic Cytology and Pathology* **35**, 235–243.

Chavez-Munguia B, Omana-Molina M, Gonzalez-Lazaro M, Gonzalez-Robles A, Cedillo-Rivera R, Bonilla P and Martinez-Palomo A (2007) Ultrastructure of cyst differentiation in parasitic protozoa. *Parasitology Research* **100**, 1169–1175.

Deutsch K and Zaman V (1959) An electron microscopic study of *Entamoeba invadens* Rodhain 1934. *Experimental Cell Research* **17**, 310–319.

Eichinger D (1997) Encystation of *Entamoeba* parasites. *Bioessays* **19**, 633–639.

Gonzalez-Salazar F, Viader-Salvado JM, Martinez-Rodriguez HG, Campos-Gongora E, Mata-Cardenas BD and Said-Fernandez S (2000) Identification of seven chemical factors that favor high-quality *Entamoeba histolytica* cyst-like structure formation under axenic conditions. *Archives of Medical Research* **31**, S192–S193.

Ludvik J and Shipstone AC (1970) The ultrastructure of *Entamoeba histolytica*. *Bulletin of the World Health Organization* **43**, 301–308.

Manna D and Singh U (2019) Nuclear factor Y (NF-Y) modulates encystation in *Entamoeba via* stage-specific expression of the NF-YB and NF-YC subunits. *mBio* **10**, e00737-19.

Mi-ichi F, Yoshida H and Hamano S (2016) Entamoeba encystation: new targets to prevent the transmission of amoebiasis. *PLoS Pathogens* **12**, e1005845.

Mi-Ichi F, Miyake Y, Tam VK and Yoshida H (2018) A flow cytometry method for dissecting the cell differentiation process of *Entamoeba encystation*. *Frontiers in cellular and infection microbiology* **8**, 250.

Mitra BN, Pradel G, Frevert U and Eichinger D (2010) Compounds of the upper gastrointestinal tract induce rapid and efficient excystation of *Entamoeba invadens*. *International Journal for Parasitology* **40**, 751–760.

Osada M (1959) Electron-microscopic studies on protozoa I. Fine structure of *Entamoeba histolytica*. *Keio Journal of Medicine* **8**, 99–103.

Picazarri K, Nakada-Tsukui K and Nozaki T (2008) Autophagy during proliferation and encystation in the protozoan parasite *Entamoeba invadens*. *Infection and Immunity* **76**, 278–288.

Picazarri K, Nakada-Tsukui K, Tsuboi K, Miyamoto E, Watanabe N, Kawakami E and Nozaki T (2015) Atg8 is involved in endosomal and phagosomal acidification in the parasitic protist *Entamoeba histolytica*. *Cellular Microbiology* **17**, 1510–1522.

Proctor EM and Gregory MA (1972) The ultrastructure of axenically cultivated trophozoites of *Entamoeba histolytica* with particular reference to an observed variation in structural pattern. *Annals of Tropical Medicine & Parasitology* **66**, 335–338.

Proctor EM and Gregory MA (1973) Ultrastructure of cysts of *E. histolytica*. *International Journal for Parasitology* **3**, 455–456.

Quach J, St-Pierre J and Chadee K (2014) The future for vaccine development against *Entamoeba histolytica*. *Human Vaccines & Immunotherapeutics* **10**, 1514–1521.

Ralston KS and Petri WA (2011) The ways of a killer: how does *Entamoeba histolytica* elicit host cell death? *Essays in Biochemistry* **51**, 193–210.

Said-Fernandez S, Campos-Gongora E, Gonzalez-Salazar F, Martinez-Rodriguez HG, Vargas-Villarreal J and Viader-Salvado JM (2001) Mg^{2+}, Mn^{2+}, and Co^{2+} stimulate *Entamoeba histolytica* to produce chitin-like material. *Journal of Parasitology* **87**, 919–923.

Saito-Nakano Y, Yasuda T, Nakada-Tsukui K, Leippe M and Nozaki T (2004) Rab5-associated vacuoles play a unique role in phagocytosis of the enteric protozoan parasite *Entamoeba histolytica*. *Journal of Biological Chemistry* **279**, 49497–49507.

Samanta SK and Ghosh SK (2012) The chitin biosynthesis pathway in *Entamoeba* and the role of glucosamine-6-P isomerase by RNA interference. *Molecular and Biochemical Parasitology* **186**, 60–68.

Samuelson J, Bushkin GG, Chatterjee A and Robbins PW (2013) Strategies to discover the structural components of cyst and oocyst walls. *Eukaryotic Cell* **12**, 1578–1587.

Siddiqui WA and Rudzinska MA (1963) A helical structure in ribonucleoprotein bodies of *Entamoeba invadens*. *Nature* **200**, 74–75.

Suresh S, Ehrenkaufer G, Zhang H and Singh U (2016) Development of RNA interference trigger-mediated gene silencing in *Entamoeba invadens*. *Infection and Immunity* **84**, 964–975.

Tanyuksel M and Petri WA Jr (2003) Laboratory diagnosis of amoebiasis. *Clinical Microbiology Reviews* **16**, 713–729.

Watanabe K and Petri WA Jr (2015) Molecular biology research to benefit patients with *Entamoeba histolytica* infection. *Molecular Microbiology* **98**, 208–217.

Wright R (2000) Transmission electron microscopy of yeast. *Microscopy Research and Technique* **51**, 496–510.

Zulfiqar H, Mathew G and Horrall S (2020) Amebiasis. In Horrall S (ed.), *StatPearls*. Treasure Island, FL: StatPearls Publishing LLC.

https://doi.org/10.1017/S0031182020001079 Published online by Cambridge University Press